

# A Bioinspired Active Robotic Simulator of the Human Respiratory System

Maria Elena Giannaccini<sup>1</sup> *Member, IEEE*, Andrew Hinit<sup>2</sup> *Member, IEEE*, Andrew Stinchcombe<sup>2</sup> *Member, IEEE*, Keren Yue<sup>2</sup> *Member, IEEE*, Martin Birchall<sup>3</sup> Andrew Conn<sup>4</sup> *Member, IEEE*, and Jonathan Rossiter<sup>2</sup> *Member, IEEE*,

**Abstract**—Pathologies affecting the respiratory system can lead to a debilitating decrease in quality of life and can be fatal. To test medical devices and implants for the human respiratory system, a simulation system that can reproduce multiple respiratory features is necessary. Currently available respiratory simulators only focus on reproducing flow rate profiles of breathing while coughing simulators focus on aerosol analysis. In this paper we propose a novel, bioinspired robotic simulator that can physically replicate both breathing and coughing flow rate characteristics of healthy adults. We conducted a study on 31 healthy adult participants to gather the flow rate measurement of normal breathing, deep breathing, breathing while running and coughing. Coughing flow rate profiles vary considerably between participants, making an accurate simulation of coughs a challenge. To enable cough flow rate simulation, a new methodology based on the identification of four cough phases, Attack, Decay, Sustain and Release (ADSR) and their parametrization was devised. This methodology leads to the unprecedented ability to reproduce diverse and complex coughing flow rate profiles. Our simulator is able to reproduce respiratory flows with a root mean square error (RMSE) of 1.8 L/min between normal participant breathing and its simulation, 5% of the maximum flow rate simulated for that participant (pMFR), an RMSE of 10.08 L/min for deep breathing, 18% of the pMFR and an RMSE of 13.29 L/min for exertion breathing, 17% of pMFR. For the simulation of an average cough we recorded an RMSE of 51.43 L/min, 13% of the pMFR and for a low flow rate cough an RMSE of 12.38 L/min, 9.5% of the pMFR. The presented simulator matches the fundamentals of human breathing and coughing, advancing the current capability of respiratory system simulators.

**Index Terms**—Human respiratory system, Bioinspired robotics, Breathing and Coughing Simulator, Medical devices testing.

## I. INTRODUCTION

Respiratory diseases can potentially be life-threatening, including pulmonary embolism, pneumonia, trauma, cancer, acute asthma and COVID-19. Physical simulators and models of the respiratory system possess considerable utility in evaluating new treatments and pathological investigations. Simulators improve our understanding of physiological functions, guiding therapies and clinician education [1], and facilitating the ex-vivo evaluation of new treatments, pharmaceuticals and implantable mechanical devices [2]. Physical simulators like

the one we present can in future be utilised to test the effectiveness of the increasing number of airway implants [3], masks, aerosol devices, inhalers, continuous positive airway pressure machines for sleep apnea and ventilators.

Compared to computational models, physical models can be used to test new devices in real world conditions and can be used for hands-on training with students. For example, the commercial product artiCHEST is a simulator with a three-dimensional and fully expanded lung for training endoscopic procedures [4]. Respiratory simulators can not only be used to develop therapies by providing test-beds which reproduce the functionality of the human body, but also to avoid unnecessary testing on animal models and people. Although required for some medical evaluations, it is advisable to avoid animal experimentation if reliable alternatives are available following the principle of 3 Rs (Replacement, Reduction and Refinement) [5]. The EU regulation 2019/1010/EU [6] specifically aims to curtail animal testing. These considerations spur the development and use of alternative systems such as physical simulators, which need to have a good level of accuracy in their simulations to be effective.

A full review of related works and respiratory system parameters is given below followed by a comparative analysis to the system presented.

### A. Related Work on Simulators

Physiological modelling with mechanical and mathematical models is a major focus for medical and bioengineering researchers. These models can be *in-vivo*, where animal models are used, *in-vitro*, where, for example, microfluidic technology interacts with layers of cell cultures, *in-silico*, through mathematical computational models and, finally mechanical models. *In-silico* models allow high controllability of the simulation at a lower cost than both *in-vivo* and mechanical models, but cannot be used as an interface of another physical, real-world system. To respect the 3 Rs principle, keep costs low so that the system is easily reproducible, and to aim to test physical medical devices, we selected a mechanical model for our study. In the following, we review the current state of the art of mechanical respiratory simulators.

We differentiate currently available mechanical breathing simulators based on whether they are commercial products or research platforms. Some notable examples of commercial simulators that reproduce breathing and are used to test respiratory therapy devices are the ASL 5000 Breathing Simulator

<sup>1</sup> School of Engineering, University of Aberdeen, Aberdeen, UK. <sup>2</sup>Department of Engineering Mathematics, University of Bristol and Bristol Robotics Laboratory, Bristol, UK. <sup>3</sup>Department of Otolaryngology, Head and Neck Surgery, UCL Ear Institute, University College London, London, UK. <sup>4</sup>Department of Mechanical Engineering, University of Bristol and Bristol Robotics Laboratory, Bristol, UK. Address correspondence to Maria Elena Giannaccini at elena.giannaccini@abdn.ac.uk.

This paper was submitted for review on 19th October 2022.

[7] also used for training, and the Ator labs breathing simulator [8]. Research simulator platforms base their novelty on: I) the materials they use or II) the type of participants they simulate. Examples of I) are recent simulators that feature a combination of artificial and organic components and include a system where pneumatic artificial muscles and organic lungs are used to recreate the motion and function of the diaphragm [9] and the xPULM electro-mechanical lung simulator, which combines in-silico, ex-vivo and mechanical respiratory approaches [10]. These innovative systems are able to generate realistic breathing simulation, but the use of organic tissue requires animal models and they do not reproduce coughing. Soft bellows have been used to simulate lungs in a physical model where they are surrounded by water simulating pleural and interstitial space [11], and in a soft robotic simulator that mimics respiratory motion in the liver for needle insertion procedures [12]. All these soft structures inherently imitate the compliance of lungs but they make the response dynamics hard to control accurately due to their visco-elastic bellow elements.

Examples of II) are the respiratory simulators that have been proposed to reproduce preterm pathological infants [13] and adult workers' flow patterns [14]. Many mechanical simulators use dynamically adjustable reservoirs [14]; while others use continuously variable flow generators such as radial fans [15]. All of the simulators discussed so far reproduce breathing only. An identification of parametrization variables and comparative analysis of existing mechanical simulators follows.

### B. Respiratory System Parameters

The analysis of breathing and coughing in this work is based on physiologically relevant parameters detailed in the following section. The standard respiratory measures of tidal volume, peak flow and respiratory rate are commonly used to diagnose respiratory illness [16] [17] [18] and hence were selected for this study. The tidal volume is the amount of air that circulates in or out of the lungs during a respiratory cycle while the patient breathes normally. In an average healthy adult male, the tidal volume measures around 0.5 L [16]. Tidal volume is vital to regulate the functioning of mechanical ventilation procedures [17]. Tidal breathing analysis can be used to identify children with asthma [18] [19]. The breath period is the time it takes to go through an entire breath cycle and is inversely proportional to the respiratory rate, which is the number of breaths taken per unit of time. In general, the respiratory rate is used to monitor fever and to facilitate identification of changes in physiology. The peak flow is the highest value of flow rate recorded by a flow meter during breathing. Flow tests are a well established method of monitoring asthma patients [20]. In this work, we have selected tidal volume, breath period and peak flow rate as breathing parameters.

Coughing is a defense reflex mechanism with the main purpose of removing excessive secretions and protecting the respiratory organs from aspiration of foreign bodies. The motor features of voluntary coughing are the same as those of involuntary reflex cough, and voluntary coughing can be used

for clearing airways as effectively as involuntary coughing [21]. Cough assessment is widely used as an indicator for respiratory diseases and in the management of patients. For example, cough strength, quantified using cough peak flow, is strongly associated with extubation success of intensive care patients [22].

In this study, we have selected cough volume, cough duration, peak flow rate, and cough acceleration as cough parameters. Cough volume is the volume of air expelled during the cough. Cough duration is the time between the start of the cough, at the point the flow rate reverses from inhalation to exhalation, and the end of the cough, once the flow rate has returned to zero. Peak flow is the highest value of flow rate registered by the flow meter during coughing. Cough acceleration is the ratio of cough peak flow to the corresponding time to cough peak flow, as defined in [21].

### C. Comparative Analysis to Presented Simulator

In this work we present a novel physical simulator that can replicate the flow rate profiles and characteristics of not only breathing but also coughing in healthy humans. This is possible due to the novel ADSR phase identification methodology (see Section III-A) and the parametrization used. In addition, the simulator utilises a bio-inspired design and modular components modelled on human anatomy to physically represent the larynx, trachea, bronchi and lungs. This modular approach aids the ability to use the simulator for testing medical devices. In contrast to our previous low-fidelity respiratory system simulator prototype that could produce limited flow rate patterns (triangular and square waves) [23], here we have significantly increased the accuracy and complexity of flow rate profile reproduction. The novel characterization and parametrization united with an accurate control system allows us to effectively reproduce the peaks and valleys of complex and diverse time-varying flows of breathing and coughing.

Mechanical simulators have been used to reproduce aerosols resulting from coughing [24], and to measure the size distributions of expiratory droplets expelled during coughing and speaking and the velocities of the expiration air jets of healthy volunteers [25]. However, these studies do not accurately characterise different cough flow rate profiles or identify their phases. Rather, they reproduce only the initial flow rate increase and subsequent flow rate decay [26] and focus mainly on aerosol generation. In contrast, our study uses the ADSR phase identification methodology, parametrization and a highly controllable mechanical system that allows us to accurately reproduce the four different phases of adult coughing we have identified. Accurately reproducing a cough is a complex task as there are several parameters to be simulated because coughs vary more significantly in profile between participants than breathing. This inter-participant variability is shown in our investigation. For this reason, in our work parameters such as volume, duration and flow rate are used to aid the simulation of both breathing and coughing. In addition, we identify four phases of the cough and match the behaviour of the control system to the requirements of each phase.

Due to its ability to simulate a range of coughing flow rates, our physical simulator is used to test a surgical mask

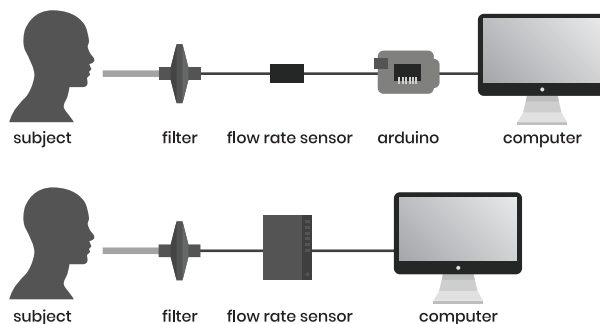


Fig. 1. Devices used for experiments with subjects. The filter is connected by an adaptor to the flow meter, which communicates with the Arduino microcontroller or directly with the PC. The setup at the top is for breathing and the setup at the bottom is for coughing.

in Section II-A. In future, it could be used to test the efficacy and reliability of multiple medical devices. For example, it could be modified to be used to test the stability of tracheal and bronchial stents at different coughing strengths. Tracheal stents may be coughed up by patients [27], which would invalidate the procedure, add risk and create discomfort. Other airway implants that could be tested by an effective physical simulator include the commercially available Spiration intrabronchial valve [28] that stops inspired air from entering the treated bronchial lobe.

This work consists of three stages: (1) a participant study and analysis of respiratory parameters, (2) design and prototyping of the simulator, and (3) testing the ability of the simulator to reproduce the flow rate profiles collected in (1). The participant study during which respiratory flow parameters are measured is described in Section II-A. The simulator is described in Section II-B. The results of the participant and simulator experiments are detailed in Section III. Finally, we discuss these results in Section IV and explain future potential applications of our simulator, aimed at progressing the fields of robotics in healthcare, in Section V.

## II. MATERIALS AND METHODS

### A. Breathing and Coughing in Subjects

In this study, we characterise breathing and coughing by recording and analysing the voluntary breathing and coughing of 31 adults.

*Participant Recruitment:* Breathing and coughing experiments were carried out with 31 healthy subjects within the age range of 18-60 years. Nine participants were female. None of the subjects had a history of cardiovascular, respiratory, neurological or any other systemic disease. The subjects were not obese and had no difficulty in performing the breathing exercises and coughing. A sensitivity analysis run by G\*Power shows that our sample of 31 participants gives us 80% power to detect medium effect sizes of at least  $d = .52$  with an alpha of  $p = .05$ . Ethics approval was granted by the Faculty of Engineering Ethics committee, University of Bristol (ID57763).

*Experiment Procedure:* All participants followed the same experimental procedures and gave informed consent to the experiments. The subjects were asked to perform three tasks

aimed at measuring their breathing patterns and then rested before performing the last task, aimed at investigating coughing patterns. Before each test, subjects were asked to sit down, fill out the ethics form and read the experiment instructions. This had the effect of settling the breathing to a relaxed pace. Each subject was seated and the procedure explained. Practice attempts were allowed. The subjects were asked to breathe normally with their mouth into the filter, connected to the measurement equipment. In addition, during the first two breathing tasks subjects were asked to pinch their nose to prevent any air leaks. The restriction was lifted for the breathing under exertion task to avoid discomfort to the participants. The tasks each subject performed were:

- T1 *Normal Breathing.* Subjects were asked to breath as naturally as they could into the flow sensor for one minute.
- T2 *Deep Breathing.* Subjects were asked to take a series of deep breaths for one minute.
- T3 *Breathing under light exertion.* Subjects were asked to breathe into the flow meter while running on the spot for one minute. No instructions were given on the level of exertion for running on the spot.
- T4 *Coughing.* Subjects were asked to take a deep breath and then cough five times consecutively into the sensor with time a short break between coughs to allow inhalation. The subjects were asked to cough as forcefully as they could, expelling as much air as possible.

The breathing and coughing experimental data was post-processed with custom-made algorithms implemented in MATLAB to consistently extract the salient breathing and coughing parameters.

*Description of the Participant Experiments Setup:* A Sensirion SFM3000 flow meter was used to measure normal breathing, deep breathing and breathing while running, and a BioPac Pneumotachometer (TSD137H) was utilised to gather coughing data. The data measured by the flow meter was collected using an Arduino Nano microcontroller, while the BioPac system uses its own data acquisition system and software (MP150). Using an Arduino and small flow meter facilitated the breathing under light exertion task as participants could hold the sensory system in their hand and were free to

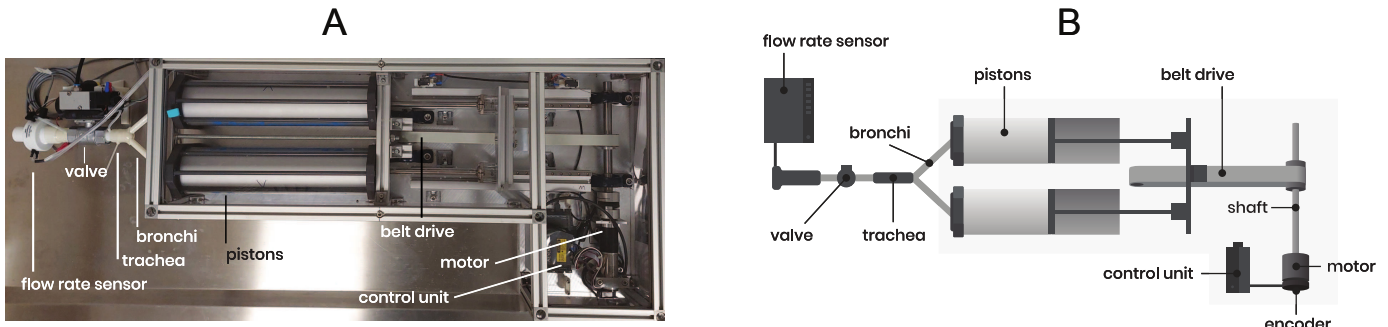


Fig. 2. A: The respiratory simulator. The outside frame ensures the safety of the simulator user. B: The components of the respiratory simulator. To generate respiration and coughing, we drive the motion of the simulator via a motor system. By varying the actuation schemes we can mimic normal, deep and light exercise breaths and coughing.

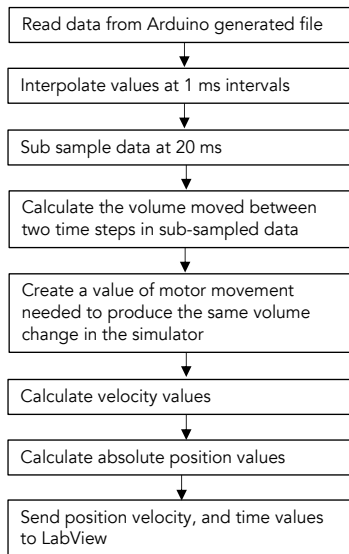


Fig. 3. Flow diagram of the details of the Python script used in the control system of the simulator.

choose the location they preferred in the room to perform the running on the spot task. This also removed any danger of the participant inadvertently displacing the tubes and wires that connect the flow sensor to its control board while running. Each participant was given a disposable anti-viral and anti-bacterial filter to prevent contaminants from each participant entering the flow meters. The transducer signals were acquired at 2 kHz. A diagram of the experimental setup is shown in Fig. 1.

**Breathing Data Processing:** The 93 total breathing patterns were analysed to identify the mean values of the three parameters: tidal volume, breath period and peak flow rate. Each of the 93 breathing patterns consists of one minute of breathing captured in the participant experiments of Section II-A. The tidal volume is the amount of air that moves in or out of the lungs in the respiratory cycle. We used the inspiration to calculate the tidal volume. The breath period is calculated as the time difference between the flow rate zero crossing at the beginning of inspiration and the zero crossing at the end of

expiration. The peak flow rate was identified by selecting the highest value of the flow rate. The raw data was smoothed using the low pass filter “fastsmooth” [29] of pseudo-Gaussian type and a mean value was calculated for each parameter for each participant.

The breath data was recorded using the SFM3000 and was already in Standard Litres Per Minute (SLPM). The breath data was recorded using an Arduino and did not need sub-sampling to be used as the input to the simulator.

**Coughing Data Processing:** In all, 155 coughs were made by 31 subjects. For each subject, the mean parameter values of the five coughs of each participant was calculated for the four parameters we utilise: volume, duration, peak flow and volume acceleration.

Cough expired volumes were calculated offline by integrating the flow rate data. For each considered cough effort, the duration was calculated as the time elapsed from the onset to end of the cough. In order to identify the start and end of the cough without errors caused by local minima the “fastsmooth” filter was applied.

In the case of single coughs where there were more than one flow rate peaks, the highest peak was chosen. The cough volume acceleration, which is the peak cough flow rate divided by time taken to reach maximum flow was also calculated.

The cough data was recorded using BioPAC in mmH<sub>2</sub>O so it required conversion to LPM to be used to drive the simulator. The cough data was recorded at 2 kHz (0.5 ms) and so needed to be sub sampled to give us 1 kHz (1 ms). The cough data required a moving average as it was noisy. We selected an 18 point moving average.

**Case Study:** A case study is performed to test the effectiveness of facemasks in reducing the amount of dispersed droplets during a cough. The simulator was used to cough onto a sheet of white paper a mixture of 1 ml water and black acrylic paint 20 cm away. The coughs were generated using participant cough data as the input to the simulator. Firstly, three coughs of varying intensity were reproduced by modifying the data from a participant’s cough. Lastly, a cough was generated with a surgical facemask (Zhende) covering the output of the simulator. In this last experiment, the amount of droplets on the paper will measure the effectiveness of the mask at inhibiting droplet projection. Each sheet of white paper with droplets was photographed and analysed to determine the extent of the

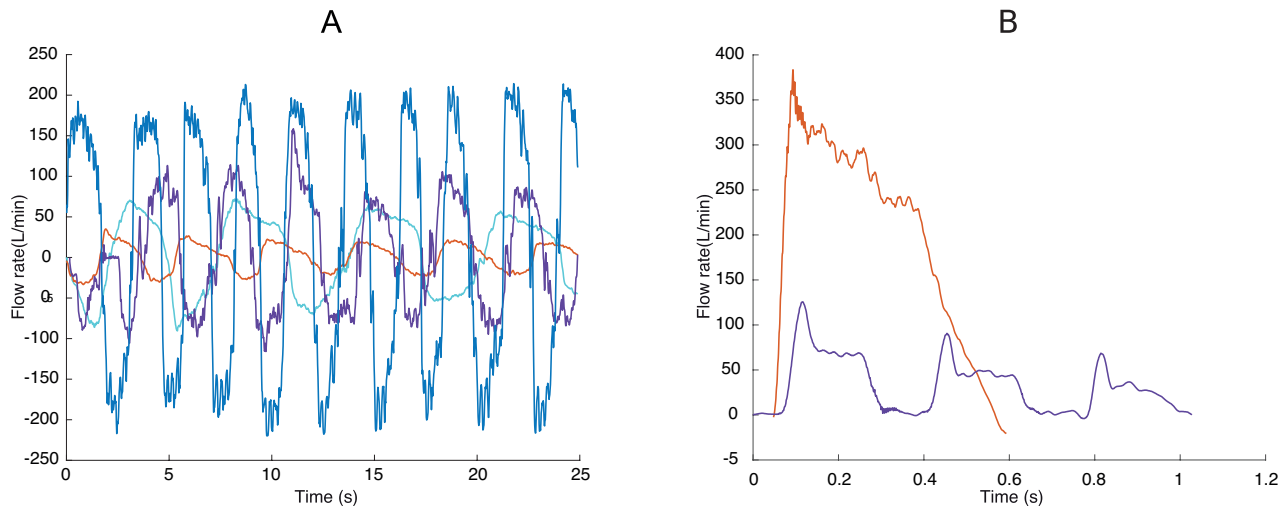


Fig. 4. Flow rate data from participants closest to mean parameter values. A: breathing data. Normal breathing data (T1, participant 24) is in orange, deep breathing (T2, participant 19) in cyan, exertion breathing (T3, participant 8) in purple and (T3, participant 12) in dark blue. B: coughing data (T4). The participant data closer to the parameter mean (participant 21) is in orange, the participant data closer to the low end of parameter values (participant 4) in purple.

TABLE I  
MEAN TIDAL VOLUME, PERIOD AND PEAK FLOW OF THE BREATH CYCLE

	Mean Volume	Mean Period	Mean Peak Flow
Normal Breathing (T1)	$0.65 \pm 0.16$ L	$4.07 \pm 0.54$ s	$28.94 \pm 5.90$ L/min
Deep Breathing (T2)	$2.1 \pm 0.24$ L	$6.30 \pm 0.59$ s	$68.08 \pm 10.76$ L/min
Exertion Breathing (T3)	$1.95 \pm 0.45$ L	$3.70 \pm 0.55$ s	$113.39 \pm 15.64$ L/min

water that had reached it. The images were converted into grayscale and their histogram was obtained using MATLAB. An algorithm based on the histogram data was used to count the number of pixels which contained the black droplets.

### B. Respiratory System Simulator

Representative samples of the acquired breathing and coughing data were chosen to test the ability of our simulator to reproduce human physiological breathing and coughing patterns. To test the simulator (Fig. 2 A) for the breathing task, the average, maximum and minimum values of the normalised three flow rate characteristics were selected. To assess the ability of the simulator to reproduce human coughing we selected the average values of the normalised four flow rate characteristics to be reproduced. The simulator was then programmed to reproduce each of these patterns. Further details on the flow rate profiles selected to be reproduced by the simulator can be found in Section III-A.

*Simulator Design:* The simulator (Fig. 2 B) features two 3-litre precision syringes/pistons (Vytalograph), which imitate the capacity of each human lung, approximately 3 litres of air in healthy adults [30]. The syringes are driven by a Maxon system including motor (EC40, 170W), with maximum motor velocity of 8000 rpm, which in the simulator corresponds to 256.44 LPM. The maximum motor acceleration is 120,000 rpm/s, which corresponds to 3846.6 LPM/s. The frequency of accelerating to maximum velocity and decelerating back to

zero velocity at 120,000rpm/s is 7.5hz. The driving system also includes a gearbox (GP42C, 74:1 reduction), encoder (HEDL 5540), and controller system (Epos 2). System stability is guaranteed by the Epos 2 motor controller. This driving system is connected to a belt transmission system. The syringes are connected to a 3D printed part modelled to mimic the “Y” shape of human upper bronchi. The average normal angle of tracheal bifurcation in human males is  $70^\circ$  and the 3D bronchi was modelled to that [31]. Average measurements and angles are used to build the bronchi and trachea so that the setup is representative of a large number of people. The diameter of the bronchi, 13mm, is modelled on the basis of male average physiological data [32], [33], [34]. The bronchi are connected to a trachea simulant, a rigid acrylic tube 19mm in diameter and 110mm long, as per physiological measures [35] [36] [37]. A simple ball valve is placed between the trachea simulant and the flow rate sensor. The valve simulates the function of the human larynx and for this reason, we refer to it as the “larynx valve”. The valve is kept open to simulate breathing and closed to allow the build-up of air pressure necessary to create a cough. The simulator control is implemented utilising three steps. First, the participant flow rate data is processed in case it is a coughing experiment, as described in Section II-A. Second, the data is fed through a Python script that calculates the position and velocity of the syringes at the right time to reproduce the participant flow rate profile (see Fig. 3). Third, the position, velocity and time data are fed to the LabView

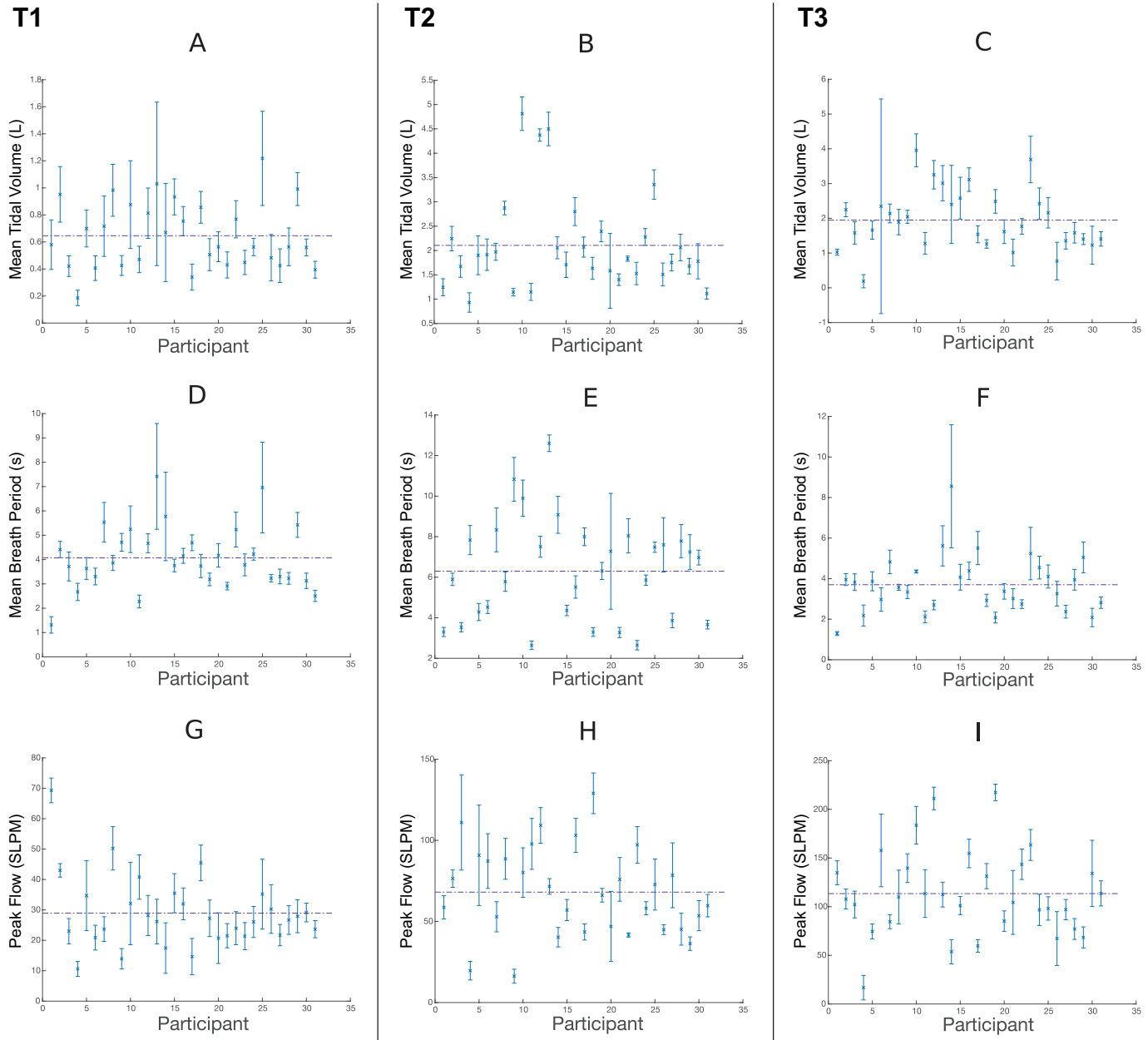


Fig. 5. Results of the data analysis in the human breathing experiments. The crosses identify participant data. The horizontal lines across the graphs represent the mean values averaged from all participants. Each point in the graphs is the average for every participant. A-C: tidal volume expressed in liters of air. D-F: period of the breathing cycle. G-I: peak flow rate. Error bars show the standard deviation for each participant. A, D, G: normal breathing (T1), B, E, H: deep breathing (T2) and C, F, I: Light exertion breathing (T3).

(National Instruments) system that then feeds it into the Epos 2, which controls the motor. This sub samples again to 20 mS samples. This is as fast as we can usefully control the simulator (due to USB). We instrumented the simulator with a flow rate sensor, a BioPac Pneumotachometer (TSD137H). The Pneumotachometer is used to measure to flow rate, which is the output of the simulator. Further details on how the system reproduces the ADSR phases are provided in Section III. The simulator is configured as a versatile platform that can be adapted to imitate both breathing and coughing profiles. Due to the modular nature of the system, specific elements

can be replaced to focus on the precise needs of different testing applications. As it has been used to test a mask in the future, we could use this simulator to evaluate the behaviour of an implantable trachea exposed to varying flow rates or enabling rapid prototyping and iterations in the design of inhalers. Currently, to the best of our knowledge, there are no other existing simulators that can capture the complex flow rate profiles of both breathing and coughing tasks.

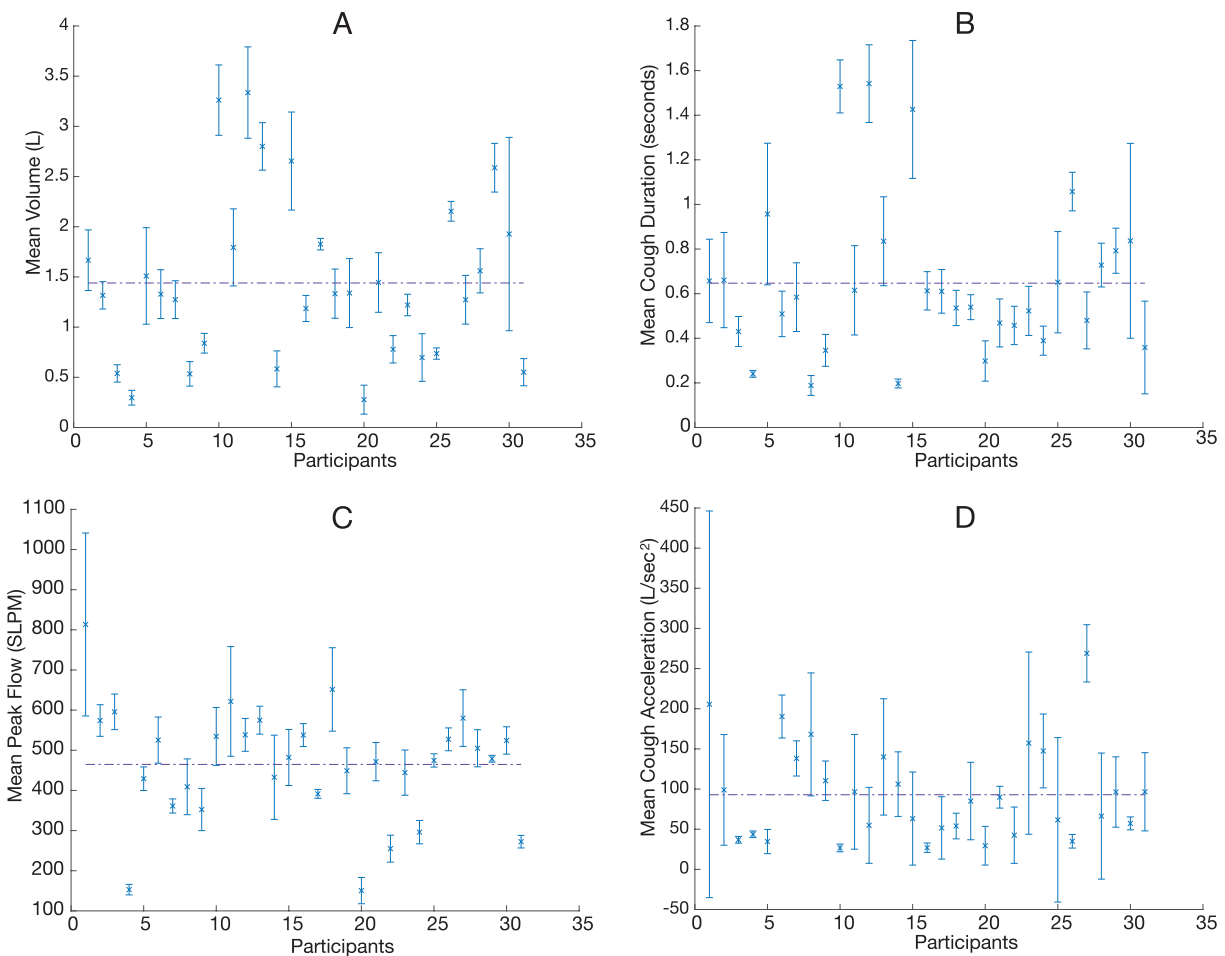


Fig. 6. Results of the data analysis in the human coughing experiments (T4). The dashed lines in the graphs represent the mean values averaged from all participants. Each point in the graphs is the average of the five coughs for every participant. A: volume of the curve underneath the cough flow rate, expressed in liters of air. B: duration of the cough event. C: peak flow rate. D: acceleration of the initial part of the cough event. For each data point error bars show the standard deviation.

### III. RESULTS

#### A. Subject Results

The next two sections detail the characteristics of the breathing and coughing profiles of the 31 healthy subjects in our experiments. Breathing profiles are shown in Fig. 4 A and coughing profiles are shown in Fig. 4 B.

*Subject Breathing Results:* As expected, the mean tidal volume increases for deep breathing and breathing during exertion compared to normal breathing (Fig. 5 and Tab. I). The mean breath period is higher for deep breaths than normal breathing but is lower for breathing while running. The mean peak flow is highest for exertion breathing and lowest for normal breathing.

The mean tidal volume value for normal breathing, 0.65L, is not significantly different from the average 0.5L value found in the literature [16]. Also, it is to be noted that in healthy adults, tidal volume measures approximately 7 mL/kg of ideal body weight [16], hence tidal volume is proportional to the body weight of participants. Between the mean normal breathing volume ( $0.65 \pm 0.16$ L) and mean exertion breathing volume ( $1.95 \pm 0.45$ L) there is a three-fold increase. The normal respiratory rate for an adult at rest is 12–18

breaths/min [38] which translates to 5–3.33 seconds for every breath cycle. These values are consistent with our finding of 4.07 s mean period value. The run-on-the-spot task (T3) was a light exercise and this is confirmed by the mean period of 3.7 s, which is consistent with the faster end of the resting breathing range. In the literature, sustained exercise is shown to cause an average of 35 breaths/min, which corresponds to a 1.7 s breath period [39]. The typical waveform of the participants' breathing pattern can be seen in Fig. 4 A.

*Subject Coughing Results:* As shown in Fig. 6 A and Tab. II, the median cough volume obtained from our analysis is  $1.44 \pm 0.24$ L. This value is consistent with the cough expired volume of 1.54L, resulting from a 700 participant study [40].

There is a strong positive correlation (correlation coefficient  $r = 0.915$ ) between the cough volume and the duration of the coughs (Fig. 6 A and B, respectively). This is intuitive, as longer coughs tend to create a higher volume of expelled air.

The cough parameter values resulting from our experiments match the values reported in the literature [41], [42]. The average peak flow rate value obtained from our analysis,  $464.8 \pm 52.6$ L/min (Fig. 6 C and Tab. II) is consistent with the values reported in the literature; a Brazilian study show that in a

TABLE II  
MEAN VOLUME, DURATION, PEAK FLOW AND ACCELERATION VALUES FOR COUGHING AND THEIR STANDARD DEVIATION

Mean Volume	Mean Duration	Mean Peak Flow	Mean Acceleration
1.44 ±0.24 L	0.65±0.14 s	464.8 ±52.6 L/min	92.9 ±46.57 L/s <sup>2</sup>

cohort of healthy subjects the peak flow rate values ranged from 240 to 500L/min [43], which also highlights the high variability in cough parameter values in different subjects. According to the literature, in healthy individuals, the average peak flow rate is higher than 300L/min in Caucasian European subjects. Further studies show that healthy subjects had a mean voluntary cough peak flow rate of 351 ±112L/min [44]. In general, the peak flow rate must be higher than 160 L/min for an effective cough [45].

Comparisons between our mean recorded cough acceleration value, 92.9 ± 46.57L/s<sup>2</sup> (Fig. 6 D), and the voluntary cough acceleration value, 199.25 ± 28.06L/s<sup>2</sup>, reported in [21] show that our result is lower. Values of mean cough acceleration of 200 ± 70L/s<sup>2</sup> in [46] confirm higher cough acceleration values than ours but also high variance. This difference in values among subjects and between cohorts of subjects is probably due to the high variability in coughing between subjects, which contributes to the challenge of designing a simulator that can reproduce human coughing.

*ADSR Phase Identification:* In music, the temporal envelope that describes how a musical note changes over time (such as a pluck of a string), can be divided into four phases: Attack, Decay, Sustain, and Release (ADSR), shown in Fig. 7 A [47]. When considering the form of the cough profile, we identified the similarity with this definition of phases resulting from the dynamics of air flow in the respiratory system. We therefore divided participant coughs into attack, decay, sustain and release phases. The phases have defined slopes of the temporal envelope, enabling discretisation of controlling parameters.

The division of the cough in the ADSR phases (Fig. 7 and Tab. III) provided an effective temporal partition of the cough with which to control the simulator. The control system parameters that can be varied are: motor velocity [*rpm*], motor acceleration [*rpm/s<sup>2</sup>*], deceleration [*rpm/s<sup>2</sup>*], overdrive distance [mm] and delay after hard valve opens and before overdrive starts [ms]. The first three are mainly determined by the motor velocity and gearbox. The fourth is limited by the length of the rail, which was chosen to allow the full extraction of the 490 mm long piston. The fifth is the ball valve closing time, which varies with the pressure in the system. The overdrive distance is the distance the syringes are pushed forwards after/during opening of the valve. The overdrive can alter attack, decay and sustain. The attack phase is successfully achieved using the delay and acceleration terms to match the peak flow rate parameter. The decay portion of the cough is successfully matched to the participant flow rate profile by altering the deceleration parameter. The duration of the cough, one of the coughing parameters shown in Fig. 6 C and Tab. II, is matched to the subject values by altering the overdrive distance. For example, for participant 21 cough simulation the overdrive distance was a linear syringe movement of 121.8 mm, which equates to 1.9 L of syringe volume displaced.

*Respiratory Simulation parametrization:* We chose to imitate the breathing patterns that are the closest to the mean of each of the key parameters recorded from participant data (listed in Tab. I). This is done for all three breathing modalities: normal breathing (T1), deep breathing (T2) and exertion breathing (T3). For coughing (T4) we reproduced the cough that is closest to the mean of the parameter values (Tab. II).

*Breathing Parameters:* The mean values of period, volume, and peak flow (Tab. I) were used to choose specific participant breathing profiles to imitate. We selected the participant closest to the average using the normalised least mean square error method. These participants were considered to best represent the mean for each of the three breathing modalities recorded because they are the most representative of the whole group of participants in our study. For normal breathing, participant 24 is chosen, with 0.56 L tidal volume, 4.23 s period and 26.04 L/min peak flow rate while the mean tidal volume value for normal breathing is 0.65 ± 0.16L, the mean period is 4.07 ± 0.54s and the peak flow rate is 28.94 ± 5.90L/min. For deep breathing, participant 19 is chosen, with 2.39 L tidal volume, 6.3 s period and 66.17 L/min peak flow rate while the mean tidal volume value for deep breathing is 2.1 ± 0.24L, the mean period is 6.30 ± 0.59s and the peak flow rate is 68.08 ± 10.76L/min. For normal breathing, participant 8 is chosen, with 1.9 L tidal volume, 3.57 s period and 109.9 L/min peak flow rate while the mean tidal volume value for exertion breathing is 1.95 ± 0.45L, the mean period is 3.7 ± 0.55s and the peak flow rate is 113.39 ± 15.64L/min. For coughing, participant 21 is chosen as they have 1.44 L volume, 0.47 s duration, 464.8 L/min peak flow, 89.83 L/sec<sup>2</sup> acceleration, which compare well with the mean values: a mean volume of 1.44±0.24L, a mean duration of 0.65±0.14s, an average peak flow rate value of 464.8 ± 52.6L/min, and a mean acceleration of 92.9 ± 46.57L/s<sup>2</sup>. We also tested the simulator with the maximum volume and flow rate recorded in the participant experiments (participant 12) to confirm its capability to reproduce the highest values recorded in our participant experiments.

*Coughing Parameters:* Medical research suggests that it is important to look at the profile of the flow rate in coughing [48], [49]. For this reason in our cough analysis we have used both the cough parameters most commonly used in the literature and the parametrization of flow rate profiles utilising the attack, decay, sustain and release model explained in Section III-A.

The first cough to imitate was chosen from the participant whose four parameters had normalised values that were closest to the general mean value. The aim was to identify the most representative participant, which was participant 21. As each participant produced five coughs the most representative of the five coughs produced by participant 21 was selected. In



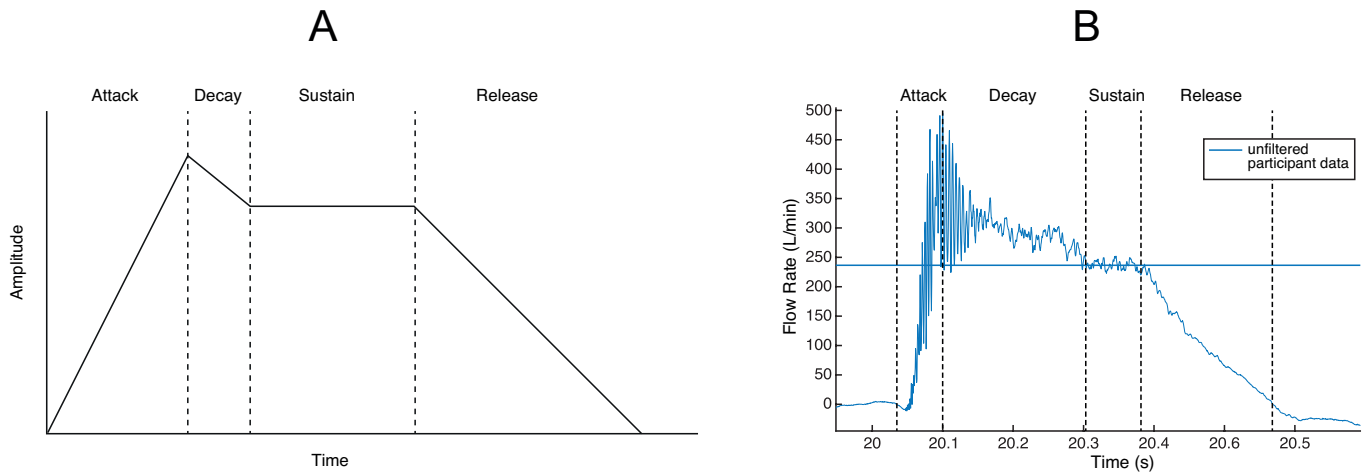


Fig. 7. A: The attack, decay, sustain, and release phases. B: The fourth cough of the set provided by participant number 21 divided into the attack, decay, sustain and release phases. The horizontal line represents the mean sustain value.

TABLE III  
DIVISION OF A COUGH FROM PARTICIPANT 21 IN THE ADSR PHASES

	Attack	Decay	Sustain	Release
Start time	20.03 s	20.1 s	20.3 s	20.38 s
Start flow rate	0.4551 L/min	494.9 L/min	245.2 L/min	228 L/min
End time	20.1 s	20.3 s	20.38 s	20.57 s
End flow rate	494.9 L/min	245.2 L/min	236.5 L/min (mean)	0.683 L/min
Slope	$110L/s^2$	$-15.65L/s^2$	0	$-20.37L/s^2$

order to reproduce this cough the larynx valve was closed and then the syringes were activated, building up air pressure, and then the larynx valve was open, releasing the pressure. This first approach produces high peak flow rates. The second approach does not use the larynx valve and can only simulate low peak flows cough profiles. In order to fully characterise the simulator behaviour both approaches were used. The second approach was used to simulate the flow rate profiles of participant 4, which have low peak flow and low acceleration.

### B. Simulator Results

*Simulator Breathing Results:* Each of the selected participant data sets was reproduced five times with the simulator. The result of the simulation of participant 24 normal breathing data (T1) compared to the participant data is shown in Fig. 8 A. The result of the simulation of participant 19 deep breathing data (T2) is compared to the participant data in Fig. 8 B. The result of the simulation of participant 8 exerted breathing data (T3) is compared to the participant data in Fig. 8 C. These figures show that the simulator closely matches the participant breathing profiles. The RMSE between the simulations and the patient data is low for normal breathing (T1) 1.8 L/min (5% of the maximum flow rate simulated for that participant), but has transient spikes during deep breathing (T2) 10.08 L/min (18% of the maximum flow rate simulated for that participant) in Fig. 8 B and exertion breathing (T3) 13.29 L/min, (17% of the maximum flow rate simulated for participant 8) in Fig. 8 C and 13.04 L/min, (6.5% of the maximum flow rate simulated for participant 12) in Fig. 8 D. As expected the error

increases due to the higher difficulty in accurately reproducing a larger and faster volume change. In all three breathing modalities the highest mean square error values correspond to the quickest changes and high magnitude changes in flow rate. In addition, the repeatability of the simulations is high with a mean standard deviation for the simulation of participant 24 breathing pattern of 0.75 L/min (2% of maximum flow rate simulated), for participant 19 breathing patterns of 1.11 L/min (1.33% of maximum flow rate simulated), for participant 8 breathing patterns of 2.82 L/min (1.88% of maximum flow rate simulated) and for participant 12 breathing patterns of 3.54 L/min (1.77% of maximum flow rate simulated).

The maximum flow rate produced by the simulator was 203.8 L/min, obtained while reproducing the exertion breathing flow profiles of participant 12 (Fig. 8 D). This participant profile displays the combination of normalised values of highest mean volume, highest mean peak flow, and lowest breathing period among the participants. This type of test is helpful to map the design envelope of the device against the requirements of the target applications.

*Simulator Coughing Results:* The cough flow rate profile of participant 21 is shown in Fig. 9. Comparison between the participant and simulator coughing profiles shows that the mean cough acceleration is higher in the simulator than in the participants. This is because the simulator has a simple open/closed larynx valve. In order to reproduce the mean cough acceleration with more accuracy, a proportional larynx valve could be used. The simulation profiles show high repeatability, as shown by the low error. In addition, the simula-

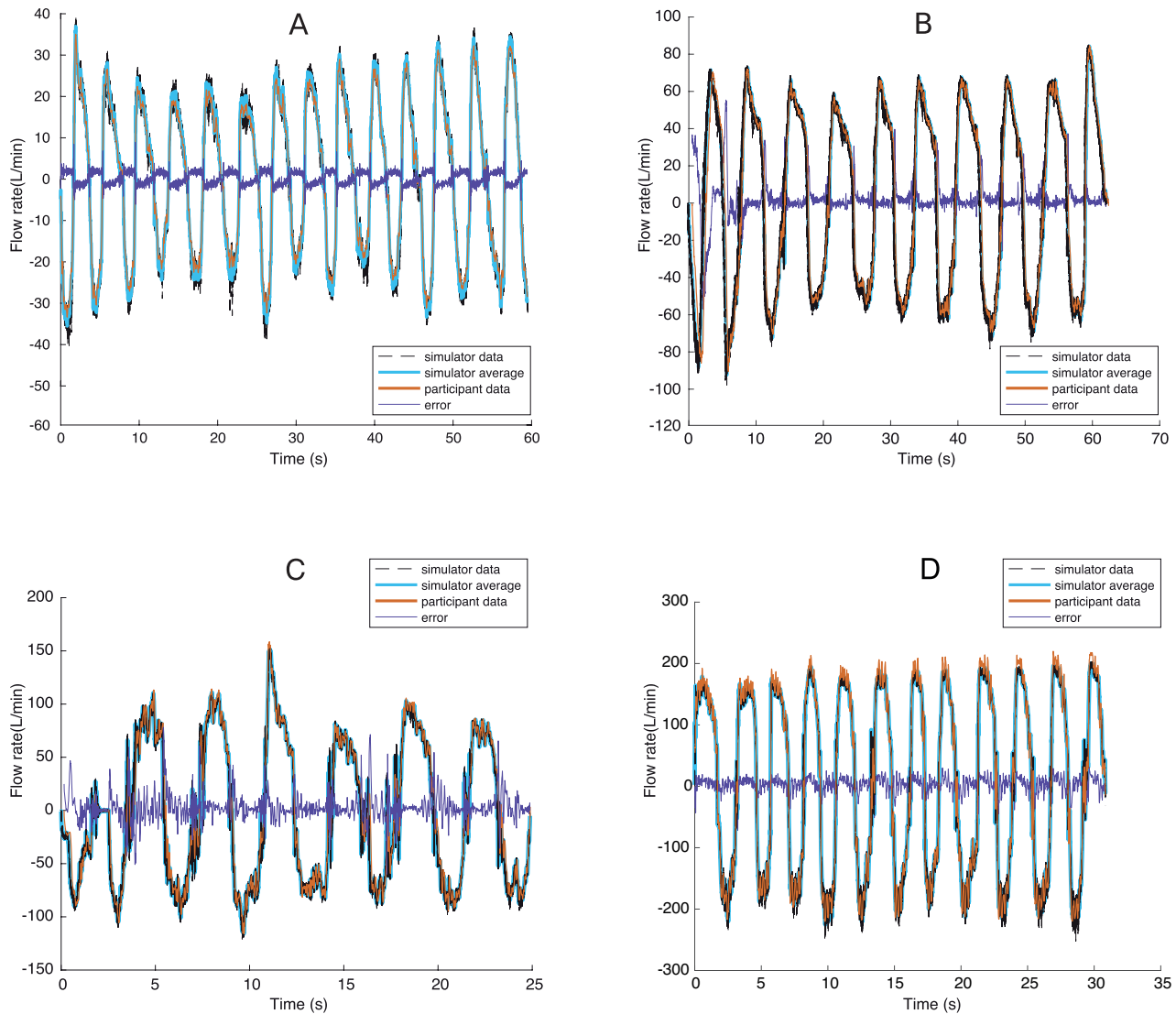


Fig. 8. Each graph shows the five simulations of breathing by a participant (in black, dashed line), their mean (in cyan) are compared to the participant data (in orange). The error between the mean simulation and the participant data is shown in purple. A: Normal breathing (T1), participant number 24. The RMSE is 1.8 L/min (5% of the maximum flow rate simulated for that participant). B: Deep breathing (T2), participant number 19. The RMSE is 10.08 L/min (18% of the maximum flow rate simulated for that participant). C: Exertion breathing (T3), participant number 8. The RMSE is 13.29 L/min (17% of the maximum flow rate simulated for that participant). D: Exertion breathing (T3), participant number 12. The RMSE is 13.04 L/min (6.5% of the maximum flow rate simulated for that participant).

tor can imitate the sequence of the four ADSR phases, which are clearly displayed in Fig. 9 A. The RMSE for this cough is 51.43L/min (13% of the maximum flow rate simulated for that participant) and the main source of this error corresponds to the attack phase just after the valve opens. For this reason we next selected a cough (from participant 4) that could be reproduced without the larynx valve to investigate whether the simulator can effectively reproduce the acceleration in the attack phase using only its motor control, i.e. without the larynx valve. The simulated cough from participant 4 is shown in Fig. 9 B. Due to the lower flow rates compared to cough 21 (Fig. 9 A), the simulator could reproduce the flow rate peaks of this cough profile without the larynx valve. This allows

a better control of the mean cough acceleration profile for a less powerful cough, compared to the the simulation using the larynx valve. This is shown by how closely the simulator emulates the highest flow rate peak of the cough (Fig. 9 B). Each of the five coughs made by participant 4 comprises three peaks, which we refer to as a triplet of coughs. The triplet shown in Fig. 9 B is the third that the participant produced. The simulator is able to recreate the cough profile well. The RMSE for this cough is 12.38L/min (9.5% of the maximum flow rate simulated for that participant) and most of this error is likely due to the negative peaks of the error in Fig. 9 B. This figure shows that the simulator reproduces double peaks in the three attack phases in the triplet cough of participant

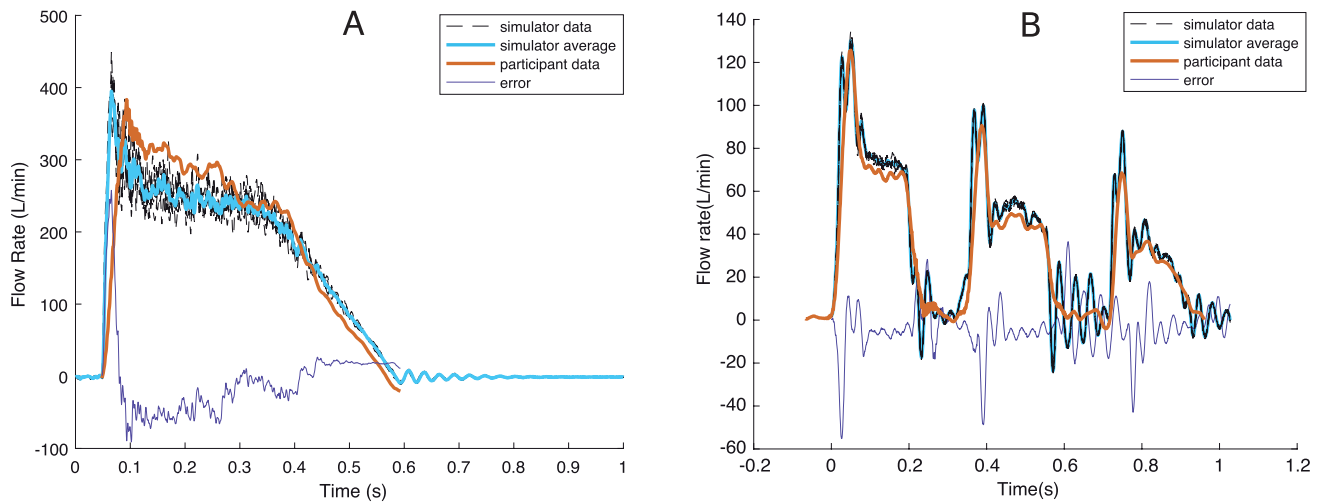


Fig. 9. The simulation of participant coughs. The outputs of the five simulations are shown in black (dashed line). The mean of these five simulations is shown in cyan. The data in orange is the participant data after applying a 18 point moving average filter, and was the input given to the simulator. The error between participant data and the average of the five simulations is shown in purple. A: simulation of a cough by participant number 21 with an RMSE of 51.43 L/min (13% of the maximum flow rate simulated for that participant) B: simulation of the third cough triplet provided by participant number 4 with an RMSE of 12.38 L/min (9.5% of the maximum flow rate simulated for that participant).

TABLE IV  
AMOUNT OF DROPLETS RESULTING FROM THE COUGH SIMULATION

	0.5 Cough Participant 4	Cough Participant 4	1.5 Cough Participant 4	Cough Participant 4 with mask
Number of pixels	2779 pixels	7332 pixels	22947 pixels	0 pixels

4, while the participant data only shows one peak for each of the three attack phases. We deduce that most of the error is due to the double peaks in the simulated data because the error (in purple in Fig. 9 B) has the highest magnitude at the same time in which the flow rate shows the double peaks Fig. 9 B also shows the high repeatability the simulator can obtain, shown by how closely the five simulations overlap. The standard deviation between the five simulations of participant 4 cough is 1.11 L/min (0.82% of maximum flow rate simulated).

*Case Study Results:* The cough profile from participant 4 (also used in Fig. 9 B) was used for the input to the simulator. In the first simulation the profile from participant 4 was used; in the second experiment the flowrate profile from participant 4 was increased by 50%; in the third experiment the same profile was decreased by 50%. As shown in Tab. IV the higher the cough flowrate profile, the larger the amount of droplets it projects. The fourth experiment used a mask. As it can be seen in Tab. IV in that case no droplets were deposited on the paper. The case study successfully showed the effectiveness of the mask to prevent the dispersion of droplets during a cough.

#### IV. DISCUSSION

The main contribution of this work is the design and characterisation of a novel simulator that can reproduce both breathing and coughing at full lung capacity (6 L). This presents an important innovation in the field of respiratory simulators, where prior simulators focussed either on breathing or on coughing [50], [8], [14], [15], [24], [51], [26]. In addition, this work contributes a novel methodology using the ADSR-based

identification of coughing phases for simulation purposes. Each cough is partitioned into four phases and reproduced through parametrization based on volume, duration, flow rate and acceleration. Using this parametrization, coughing tidal volume and mean duration can be reproduced. The on/off nature of the larynx valve used here does not replicate gradual larynx opening. The valve therefore constrains the value of flow rate acceleration.

Our cough simulation findings replicate the magnitude of the high flow rates reproduced in [26] that imitates coughing but not breathing. In [26] a simple representation of the cough flow rate profile is used. In contrast, our study successfully identified and simulated all four phases of the ADSR profile. This, as illustrated in Fig. 9, is compelling evidence that the combination of our ADSR phase classification methodology and simulator parametrization can replicate flow rate profiles of a complexity that, to the best of our knowledge, has not been attained before.

The parametrization of breathing is a contributing factor to the accuracy of the simulator in reproducing the breathing mean period and mean peak flow for normal, deep and exertion breathing, with highest accuracy for normal breathing. Existing physical breathing simulators are capable of generating only limited air flow patterns (sine, triangular and square waves) [14]. In contrast our simulator can reproduce the flow rate profiles of breathing and coughing.

A recently proposed framework has defined fidelity in physical organ simulators as identified by three main features: anatomy, physiological behavior, and materials [2]. Our sim-

ulator replicates anatomy by reproducing the correct average dimensions and general shape of the simulated trachea and bronchi. Physiological behaviour is simulated by imitating the respiratory system parameters and using syringes to imitate the average adult lung capacity (6L). We reproduce the motion and function of lungs for different breathing states and couple the syringes with a valve that imitates the larynx in order to reproduce coughing profiles.

### A. Limitations

Our simulator reproduces human respiratory flow rate profiles through control rather than by using materials similar to human tissue, whose characteristics are difficult to reproduce artificially and may be affected by environmental conditions such as temperature and humidity. Regarding the physical design of the simulator we are limited in our maximum velocity, acceleration and deceleration. We can achieve most breathing patterns within these limits but not all coughs due to their fast acceleration and peak volume. This could be improved by using more powerful motors and controllers.

The trachea and bronchi modules used were chosen to be representative of the largest number of people, which allowed us to use them to simulate the flow rates of multiple participants. However, where medical imaging of trachea and bronchi is available, participant-specific 3D prints of the two organs can be used, as suggested in [2]. This would open the way for inter-participant variability studies. In addition, detailed models of the bronchi, trachea and oral and nasal cavities would allow a more complete velocity profile of the complex air flow in the human respiratory system to be reproduced.

## V. CONCLUSION

This study demonstrates the feasibility of implementing a simulator with high reproducibility for the simulation of both full lung capacity flow rate coughing profiles with RMSE of 51.43L/min for the most average cough and flow rate breathing profiles with RMSE of 1.8 L/min between normal breathing and its simulation. This is achieved through parametrization derived from participant experiments and the ADSR cough phase identification methodology.

The evaluation of the system design has shown that the presented design, the parametrization of participant data and ADSR phase identification methodology have the potential to be a first-stage evaluative tool for the development of robotic healthcare solutions. The modular nature of the system allows the customisation of features for different applications. For example, if the aim is testing an implantable trachea, as seen in [52], the implant could be physically integrated in the simulator, thus combining the advantage of the accuracy of repetitive tests (e.g. fatigue cycle testing) with the controllability of a robotic system. Our case study successfully showed the effectiveness of the simulator in testing the ability of a surgical mask in preventing the dispersion of droplets during a cough. In addition, this simulator can test the prototypes developed in the context of the RoboVox project, which aims to design and test a novel soft robotic valve for the respiratory system

[53]. Using physical simulators, tests of medical devices could be done at an earlier development stage, with a high level of reproducibility and in an environment that can reproduce multiple respiratory system functions. This will accelerate innovation in the field of devices for the respiratory system, ultimately leading to increased patient safety and comfort.

In future, the simulator could be used to reproduce pathological breathing and coughing profiles. This would expand the spectrum of tests on medical devices that the simulator can perform and further reduce the requirement for animal or human testing. Also, simulations could be customised to the patient by using patient specific 3D moulds of trachea and bronchi. In addition, further exertion experiments could be conducted in controlled conditions, for example using a treadmill to ensure all participants run at the same velocity, to decrease the inter-participant variability.

## ACKNOWLEDGMENTS

This work was supported by funding from Wellcome Trust. JR is funded by the EPSRC through grants EP/V062158/1, EP/T020792/1, EP/V026518/1, EP/S026096/1 and EP/R02961X/1 and the Royal Academy of Engineering as Chair of Emerging Technologies. AC is funded by the EPSRC through grants EP/T020792/1 and EP/R02961X/1. In addition we would like to thank Gravestone J. for his insights, Bennett G. for his vital help with graphics, Cadegiani A. for her longstanding help with mathematics, Prof. P. Back for his help with statistics and Paulraj R. from UCLB.

*Conflict of Interest:* There are no conflicts of interest in this study.

*Data Access Statement:* The datasets have been deposited in the University of Bristol repository.

## REFERENCES

- [1] N. R. MacIntyre, "Respiratory system simulations and modeling," *Respiratory care*, vol. 49, no. 4, pp. 401–409, 2004.
- [2] S. Maglio, C. Park, S. Tognarelli, A. Mencias, and E. Roche, "High fidelity physical organ simulators: from artificial to bio hybrid solutions," *IEEE Transactions on Medical Robotics and Bionics*, 2021.
- [3] S. A. Roodenburg, S. D. Pouwels, and D.-J. Slebos, "Airway granulation response to lung-implantable medical devices: a concise overview," *European Respiratory Review*, vol. 30, no. 161, 2021.
- [4] J. Biederer and M. Heller, "Artificial thorax for mr imaging studies in porcine heart-lung preparations," *Radiology*, vol. 226, no. 1, pp. 250–255, 2003.
- [5] W. M. S. Russell and R. L. Burch, *The principles of humane experimental technique*. Methuen, 1959.
- [6] E. Parliament, "Regulation 2019/1010 - on the alignment of reporting obligations in the field of legislation related to the environment, and amending regulations (ec)," *No 166/2006 and (EU) No 995/2010 of the European Parliament and of the Council, Directives 2002/49/EC, 2. Off. J. Eur. Union*, pp. 115–127, 2019.
- [7] I. Medical, "Asl 5000 breathing simulator." 2022, [Online; accessed June 29, 2022]. [Online]. Available: [\url{https://www.ingarmed.com/product/asl-5000-breathing-simulator/}](https://www.ingarmed.com/product/asl-5000-breathing-simulator/)
- [8] A. labs, "The abms system, automated breathing metabolic simulator." 2022, [Online; accessed June 29, 2022]. [Online]. Available: [\url{https://atorilabs.com/abms-platform/}](https://atorilabs.com/abms-platform/)
- [9] M. A. Horvath, L. Hu, T. Mueller, J. Hochstein, L. Rosalia, K. A. Hibbert, C. C. Hardin, and E. T. Roche, "An organosynthetic soft robotic respiratory simulator," *APL Bioengineering*, vol. 4, no. 2, p. 026108, 2020.
- [10] R. Pasteka, M. Forjan, S. Sauermaun, and A. Drauschke, "Electromechanical lung simulator using polymer and organic human lung equivalents for realistic breathing simulation," *Scientific Reports*, vol. 9, no. 1, pp. 1–12, 2019.

- [11] A. Verbraak, J. Beneken, J. Bogaard, and A. Versprille, "Computer-controlled mechanical lung model for application in pulmonary function studies," *Medical and Biological Engineering and Computing*, vol. 33, no. 6, pp. 776–783, 1995.
- [12] H. Naghibi, P. A. Costa, and M. Abayazid, "A soft robotic phantom to simulate the dynamic respiratory motion of human liver," in *2018 7th IEEE international conference on biomedical robotics and biomechanics (Biorob)*. IEEE, 2018, pp. 577–582.
- [13] I. Baldoli, A. Cuttano, R. T. Scaramuzzo, S. Tognarelli, M. Ciantelli, F. Cecchi, M. Gentile, E. Sigali, C. Laschi, P. Ghirri *et al.*, "A novel simulator for mechanical ventilation in newborns: Mechatronic respiratory system simulator for neonatal applications," *Proceedings of the Institution of Mechanical Engineers, Part H: Journal of Engineering in Medicine*, vol. 229, no. 8, pp. 581–591, 2015.
- [14] H. Yuasa, M. Kumita, T. Honda, K. Kimura, K. Nozaki, H. Emi, and Y. Otani, "Breathing simulator of workers for respirator performance test," *Industrial health*, 2014.
- [15] F. Bautsch, G. Männel, and P. Rostalski, "Development of a novel low-cost lung function simulator," *Current Directions in Biomedical Engineering*, vol. 5, no. 1, pp. 557–560, 2019.
- [16] S. Hallett and J. V. Ashurst, "Physiology, tidal volume," in *StatPearls [Internet]*. StatPearls Publishing, 2019.
- [17] S. W. Salyer, *Essential emergency medicine: for the healthcare practitioner*. Elsevier Health Sciences, 2007.
- [18] K. Carlsen and K. L. Carlsen, "Tidal breathing analysis and response to salbutamol in awake young children with and without asthma," *European Respiratory Journal*, vol. 7, no. 12, pp. 2154–2159, 1994.
- [19] H. Hmeidi, S. Motamedi-Fakhr, E. Chadwick, F. J. Gilchrist, W. Lenney, R. Iles, R. C. Wilson, and J. Alexander, "Tidal breathing parameters measured using structured light plethysmography in healthy children and those with asthma before and after bronchodilator," *Physiological reports*, vol. 5, no. 5, p. e13168, 2017.
- [20] T. Clark and M. Hetzel, "Diurnal variation of asthma," *British journal of diseases of the chest*, vol. 71, pp. 87–92, 1977.
- [21] G. A. Fontana, T. Pantaleo, F. Lavorini, D. Mutolo, G. Polli, and M. Pistolesi, "Coughing in laryngectomized patients," *American journal of respiratory and critical care medicine*, vol. 160, no. 5, pp. 1578–1584, 1999.
- [22] C. Jiang, A. Esquinas, and B. Mina, "Evaluation of cough peak expiratory flow as a predictor of successful mechanical ventilation discontinuation: a narrative review of the literature," *Journal of intensive care*, vol. 5, no. 1, p. 33, 2017.
- [23] M. E. Giannaccini, K. Yue, J. Graveston, M. Birchall, A. Conn, and J. Rossiter, "Respiratory simulator for robotic respiratory tract treatments," in *2017 IEEE International Conference on Robotics and Biomimetics (ROBIO)*. IEEE, 2017, pp. 2314–2319.
- [24] M. Seaver, J. D. Eversole, J. J. Hardgrove, W. K. Cary, and D. C. Roselle, "Size and fluorescence measurements for field detection of biological aerosols," *Aerosol Science and technology*, vol. 30, no. 2, pp. 174–185, 1999.
- [25] C. Y. H. Chao, M. P. Wan, L. Morawska, G. R. Johnson, Z. Ristovski, M. Hargreaves, K. Mengersen, S. Corbett, Y. Li, X. Xie *et al.*, "Characterization of expiration air jets and droplet size distributions immediately at the mouth opening," *Journal of aerosol science*, vol. 40, no. 2, pp. 122–133, 2009.
- [26] W. G. Lindsley, J. S. Reynolds, J. V. Szalajda, J. D. Noti, and D. H. Beezhold, "A cough aerosol simulator for the study of disease transmission by human cough-generated aerosols," *Aerosol Science and Technology*, vol. 47, no. 8, pp. 937–944, 2013.
- [27] S. A. Zakaluzny, J. D. Lane, and E. A. Mair, "Complications of tracheo-bronchial airway stents," *Otolaryngology—Head and Neck Surgery*, vol. 128, no. 4, pp. 478–488, 2003.
- [28] Olympus, "Spiration valve system for treatment of severe emphysema." 2022, [Online; accessed July 21, 2022]. [Online]. Available: [\url{https://medical.olympusamerica.com/products/spiration-valve-system-treatment-severe-emphysema}](https://medical.olympusamerica.com/products/spiration-valve-system-treatment-severe-emphysema)
- [29] T. O'Haver, "Fast smoothing function, matlab central file exchange." 2022, [Online; accessed February 10, 2022]. [Online]. Available: [\url{https://www.mathworks.com/matlabcentral/fileexchange/19998-fast-smoothing-function}](https://www.mathworks.com/matlabcentral/fileexchange/19998-fast-smoothing-function)
- [30] B. J. Delgado and T. Bajaj, "Physiology, lung capacity," 2019.
- [31] S. M. Alavi, T. E. Keats, and O. W. M., "The angle of tracheal bifurcation: its normal mensuration," *American Journal of Roentgenology*, vol. 108, no. 3, pp. 546–549, 1970.
- [32] D. Kim, J.-S. Son, S. Ko, W. Jeong, and H. Lim, "Measurements of the length and diameter of main bronchi on three-dimensional images in asian adult patients in comparison with the height of patients," *Journal of cardiothoracic and vascular anesthesia*, vol. 28, no. 4, pp. 890–895, 2014.
- [33] J. W. Lee, J.-S. Son, J.-W. Choi, Y.-J. Han, and J.-R. Lee, "The comparison of the lengths and diameters of main bronchi measured from two-dimensional and three-dimensional images in the same patients," *Korean journal of anesthesiology*, vol. 66, no. 3, p. 189, 2014.
- [34] T. Hampton, S. Armstrong, and W. Russell, "Estimating the diameter of the left main bronchus," *Anaesthesia and intensive care*, vol. 28, no. 5, pp. 540–542, 2000.
- [35] S. Sakuraba, R. Serita, J. Kuribayashi, S. Kosugi, H. Arisaka, K. Yoshida, and J. Takeda, "Comparison of tracheal diameter measured by chest x-ray and by computed tomography," *Anesthesiology research and practice*, vol. 2010, 2010.
- [36] E. Breatnach, G. C. Abbott, and R. G. Fraser, "Dimensions of the normal human trachea," *American Journal of Roentgenology*, vol. 142, no. 5, pp. 903–906, 1984.
- [37] U. Cinar, S. Halezeroglu, E. Okur, M. A. Inanici, and S. Kayaoglu, "Tracheal length in adult human: the results of 100 autopsies," *Int. j. morphol.*, vol. 34, no. 1, pp. 232–236, 2016.
- [38] K. E. Barrett, S. M. Barman, H. L. Brooks, and J. X.-J. Yuan, *Ganong's review of medical physiology*. McGraw-Hill Education, 2019.
- [39] A. Nicolò, C. Massaroni, and L. Passfield, "Respiratory frequency during exercise: the neglected physiological measure," *Frontiers in physiology*, vol. 8, p. 922, 2017.
- [40] S. Ren, J. Niu, Z. Luo, Y. Shi, M. Cai, Z. Luo, and Q. Yu, "Cough expired volume and cough peak flow rate estimation based on ga-bp method," *Complexity*, vol. 2020, 2020.
- [41] A. Nunn and I. Gregg, "New regression equations for predicting peak expiratory flow in adults," *BMJ*, vol. 298, no. 6680, pp. 1068–1070, 1989.
- [42] A. Beardsell, S. Bell, S. Robinson, and H. Rumbold, "Mcm part a: Mcqs," *Royal Society of Medicine Press*, p. 2009, 2009.
- [43] F. E. Cardoso, L. C. de Abreu, R. D. Raimundo, N. A. Faustino, S. F. Araújo, V. E. Valenti, M. A. Sato, S. R. Martins, and J. A. Torquato, "Evaluation of peak cough flow in brazilian healthy adults," *International archives of medicine*, vol. 5, no. 1, p. 25, 2012.
- [44] F. Harraf, K. Ward, W. Man, G. Rafferty, K. Mills, M. Polkey, J. Moxham, and L. Kalra, "Transcranial magnetic stimulation study of expiratory muscle weakness in acute ischemic stroke," *Neurology*, vol. 71, no. 24, pp. 2000–2007, 2008.
- [45] L. M. Gauld and A. Boynton, "Relationship between peak cough flow and spirometry in duchenne muscular dystrophy," *Pediatric pulmonology*, vol. 39, no. 5, pp. 457–460, 2005.
- [46] K. Ward, J. Seymour, J. Steier, C. Jolley, M. Polkey, L. Kalra, and J. Moxham, "Acute ischaemic hemispheric stroke is associated with impairment of reflex in addition to voluntary cough," *European Respiratory Journal*, vol. 36, no. 6, pp. 1383–1390, 2010.
- [47] J. J. Burred, A. Robel, and T. Sikora, "Dynamic spectral envelope modeling for timbre analysis of musical instrument sounds," *IEEE Transactions on Audio, Speech, and Language Processing*, vol. 18, no. 3, pp. 663–674, 2009.
- [48] M. Chaudri, C. Liu, R. Hubbard, D. Jefferson, and W. Kinnear, "Relationship between supramaximal flow during cough and mortality in motor neurone disease," *European Respiratory Journal*, vol. 19, no. 3, pp. 434–438, 2002.
- [49] A. Szeinberg, E. Tabachnik, N. Rashed, F. J. McLaughlin, S. England, C. A. Bryan, and H. Levison, "Cough capacity in patients with muscular dystrophy," *Chest*, vol. 94, no. 6, pp. 1232–1235, 1988.
- [50] O. incorporated, "Breathing simulator." 2022, [Online; accessed June 29, 2022]. [Online]. Available: [\url{https://www.ocenco.com/products/breathing-simulator/}](https://www.ocenco.com/products/breathing-simulator/)
- [51] W. G. Lindsley, J. D. Noti, F. M. Blachere, J. V. Szalajda, and D. H. Beezhold, "Efficacy of face shields against cough aerosol droplets from a cough simulator," *Journal of occupational and environmental hygiene*, vol. 11, no. 8, pp. 509–518, 2014.
- [52] C. Crowley, M. Birchall, and A. M. Seifalian, "Trachea transplantation: from laboratory to patient," *Journal of Tissue Engineering and Regenerative Medicine*, vol. 9, no. 4, pp. 357–367, 2015.
- [53] RoboVox, "Robovox," 2022, [Online; accessed Dec 18, 2022]. [Online]. Available: [\url{https://www.ucl.ac.uk/surgery/research/research-department-orthopaedics-and-musculoskeletal-science/aspire-create/research-16}](https://www.ucl.ac.uk/surgery/research/research-department-orthopaedics-and-musculoskeletal-science/aspire-create/research-16)